

Original Article

Proposal of an improved histological sub-typing system for lung adenocarcinoma – significant prognostic values for stage I disease

Koji Okudela^{*1}, Tetsukan Woo^{*2}, Hideaki Mitsui¹, Takuya Yazawa¹, Hiroaki Shimoyamada¹, Michihiko Tajiri³, Nobuo Ogawa³, Munetaka Masuda², and Hitoshi Kitamura¹

Department of ¹Pathology and ²Surgery, Yokohama City University Graduate School of Medicine, Yokohama, Japan; ³Division of General Thoracic Surgery, Kanagawa Prefectural Cardiovascular and Respiratory Center Hospital, Yokohama, Japan. *The authors equally contributed to this work.

Received March 19, 2010, accepted March 21, 2010, available online: March 25, 2010

Abstract: We have established a concise sub-typing system suitable for predicting the postoperative outcome in cases of stage I lung adenocarcinoma (ADC), using morphometric profiling. The association between postoperative disease recurrence and a variety of morphological features including histological architecture, cell type, cytoplasmic color/internal structure, nuclear shape/size, chromatin pattern, and nucleoli count/remarkableness, was analyzed. Histological architecture had the most prognostic value and could be subdivided into low-grade (bronchioloalveolar, papillary and tubular: “tubular” in this paper is defined as a tubular or glandular structure lined with single-layered neoplastic cells) and high-grade (acinar and solid: “acinar” is defined as a tubular or glandular structure lined with poly-layered neoplastic cells or as a fused glandular structure such as the cribriform pattern) components. The sub-groups separated based on a cut-off value, 71.5% of the high-grade component comprised by a tumor, which was calculated according to a relative operating characteristic curve, exhibited a significant difference in disease recurrence [estimated 5-year disease-free survival rate, 95.3% in the low-grade group versus 66.7% in the high-grade group, hazard ratio 7.35, Log-rank test $p = 0.002$]. The sub-grouping system is concise and suitable for practical use. It will improve the histological classification of ADC.

Keywords: Lung adenocarcinoma, stage I, morphometric profiling, altered sub-typing system, prognostic value

Introduction

Lung cancer is a leading cause of cancer-related deaths in the developed world [1,2]. Adenocarcinoma (ADC) is the most common histological type and even tumors without nodal metastasis (stage I disease) can be fatal [2,3,4,5,6,7]. Recent studies reported a beneficial effect of adjuvant chemotherapy on survival in a poor prognostic group of patients with stage I ADC [8,6,9]. The accurate identification of tumors having the potential to recur and selection of an appropriate adjuvant therapy would improve postoperative performance. Histological appearance is one indicator of postoperative outcome [2,4,10]. The World Health Organization (WHO) has further classified ADC into five

sub-types, bronchioloalveolar, acinar, papillary, solid, and mixed, the latter consisting different sub-types [2]. Although this sub-typing has been widely adopted, it has a crucial flaw in that most ADCs (more than 80%) are inevitably categorized as mixed because they usually consist of highly heterogeneous components [2]. Actually, clinical course seems to vary among individuals with the mixed ADC even at an identical stage. Our recent study has established a novel system using morphometric profiling to subdivide mixed ADC and demonstrated its potential prognostic value [10]. However, the system was too complex in methodology to be widely adopted for clinical use [10]. The present study has tried to identify the morphometric element most closely associated with the postoperative out-

come of ADC at stage I, and succeeded in establishing a concise sub-typing system suitable for practical use.

Materials and methods

Primary lung cancers

All 187 patients with ADC underwent radical surgical resection at Kanagawa Prefectural Cardiovascular and Respiratory Center Hospital (Yokohama, Japan) between January 2001 and December 2006. Every tumor examined was at stage I according to the international TNM classification system [11]. Among the 187 ADCs, 130 were at stage IA (T1N0M0; T1, tumor less than or equal to 30mm in the maximal diameter) and 57 were at stage IB (T2N0M0; T2, tumor more than 30mm in the maximal diameter or one with pleural invasion), respectively. One, 165, and 6 patients underwent a pneumonectomy, lobectomy, and segmentectomy, along with a lymphadenectomy extending to the hilar and mediastinal lymph nodes, respectively. Fifteen patients underwent a wedge resection along with lymph-node sampling. A follow-up evaluation was performed every 2 months for the first 2 years after the operation, every 3 months in the third year, and every 6 months thereafter. The evaluation included physical examinations and chest radiography. An examination using serum tumor markers, computed tomography of the thorax and upper abdomen, and magnetic resonance imaging of the brain were performed every 6 months for the first 3 years, and every 12 months thereafter. In the analyses for DFS, recurrence ratio and hazard ratio, SQCs were excluded. The median follow-up period was 35.9 (range, 1.1 to 82.5) months. The post-operative disease-free span was defined as the period ranging from the date of surgical operation to the date when the recurrence of disease was diagnosed. An observation was censored at the last follow-up if the patient was alive or had died of a cause other than lung cancer. The median disease-free span was 11.8 (range, 3.8 to 49.1) months for patients with recurrent disease, and 36.2 (range, 1.1 to 82.5) months for those without recurrent disease. None of the patients with stage IA disease, and 19 of 57 patients with stage IB disease received postoperative adjuvant chemotherapy (3 patients received cisplatin or carboplatin-based chemotherapy, and 16 patients received oral uracil-tegafur (UFT) chemotherapy). The 5-year

disease-free survival (DFS) rate was 65.4% for the non-adjuvant stage IB group versus 66.0% for the adjuvant stage IB group ($P=0.8057$, 4 patients who could not continue oral UFT treatment for more than 6 months were excluded). Ethics committees of both Yokohama City University and Kanagawa Prefectural Cardiovascular and Respiratory Center Hospital approved the protocol of this work. Informed consent to use the resected materials for research was obtained from all the subjects.

Morphometric features

Morphological elements were defined as in our previous study [10] but a few modifications. Histological architecture was subdivided into 10 patterns, (1) bronchioalveolar (BAC), (2) tubular (TUB), (3) acinar (ACN), (4) ductular (DCT), (5) trabecular (TRB), (6) papillary (PAP), (7) solid (SOL), (8) single (SGR), (9) striated (STR), and (10) neuroendocrinal (NER). The BAC pattern was defined as an extension of neoplastic cells on proper alveolar septa (**Figure 1**), the TUB pattern as a tubular or glandular structure lined with single-layered epithelial cells (**Figure 1**), the ACN pattern was as a tubular or glandular structure lined with poly-layered epithelial cells or as a fused glandular structure such as the cribriform pattern (**Figure 1**), the TRB pattern as a line of single neoplastic cells connected like a train (**Figure 1**), the PAP pattern as an extension of neoplastic cells on fibrotic stalks like papillae (**Figure 1**), the SOL pattern as the formation of solid nests consisting of neoplastic cells (**Figure 1**), the SGL pattern as an extension of unconnected neoplastic cells (**Figure 1**), the STR pattern as the striation of neoplastic cells like the striated squamous epithelium (**Figure 1**), and the NER pattern as an architecture showing some neuroendocrinal features such as roset and cord/ribbon-like structures (**Figure 1**). Cell type was classified as follows, (1) high columnar (HCL), (2) low columnar (LCL), (3) spheroid (SPH), (4) hobnail (HOB), (5) polygonal (PLG), (5) global (GLB), small round (SMR), and (8) spindle (SPN). HCL was defined as resembling bronchial surface epithelial cells (**Figure 2**), LCL as resembling non-ciliated bronchiolar epithelial cells (**Figure 2**), SPH as resembling type II pneumocytes (**Figure 2**), HOB as showing features intermediate between those of type II pneumocytes and non-ciliated bronchiolar epithelial cells (**Figure 2**), PLG as having a polygonal appearance with ob-

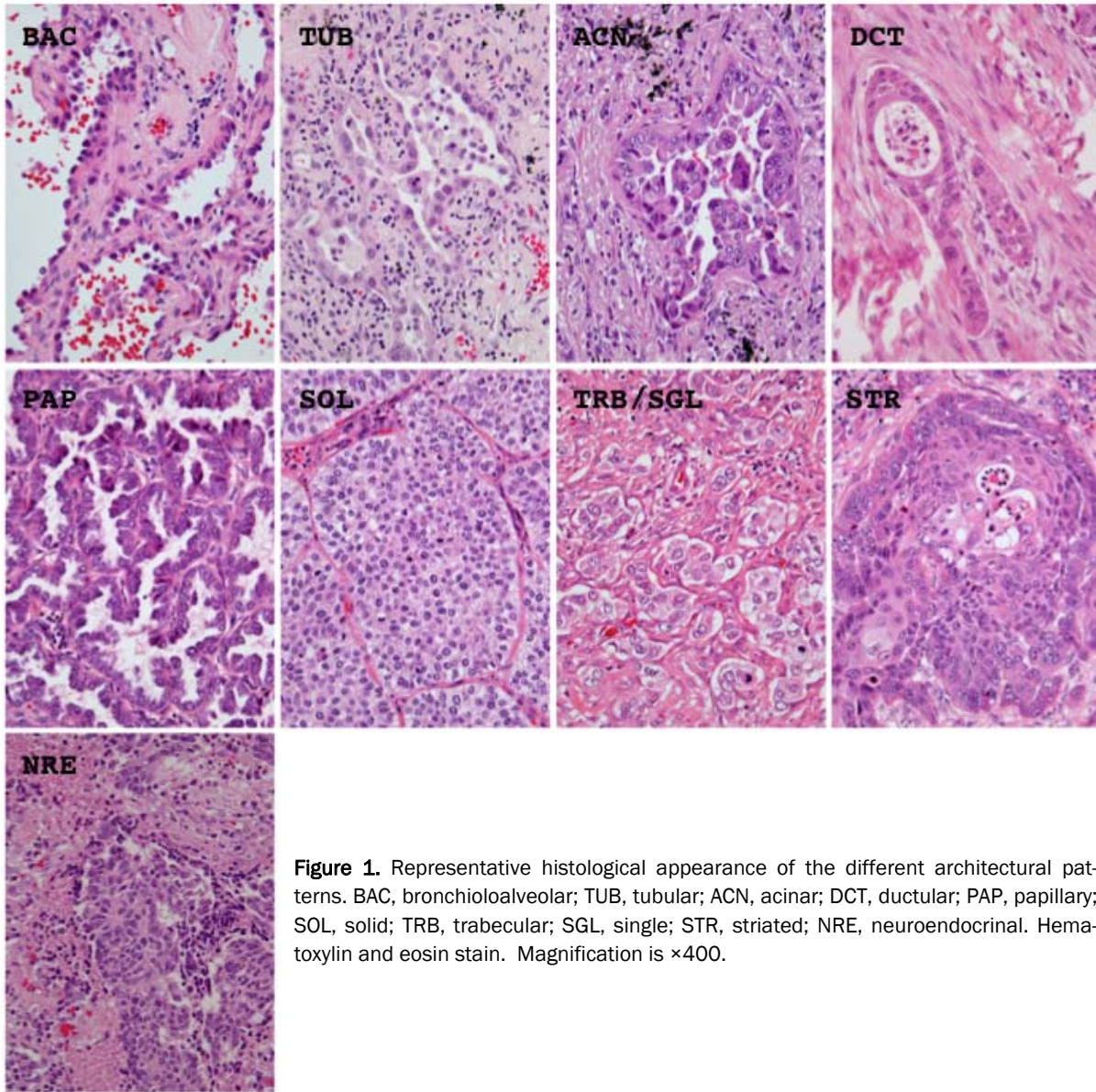


Figure 1. Representative histological appearance of the different architectural patterns. BAC, bronchioloalveolar; TUB, tubular; ACN, acinar; DCT, ductular; PAP, papillary; SOL, solid; TRB, trabecular; SGL, single; STR, striated; NRE, neuroendocrinal. Hematoxylin and eosin stain. Magnification is $\times 400$.

vious cell-cell adherence (**Figure 2**), GLB as having a global appearance without obvious cell-cell adherence (**Figure 2**), SMR as having a small round or oat-like appearance with scant cytoplasm (**Figure 2**), and SPN as resembling spindle-shaped mesenchymal cells (**Figure 2**). Cytoplasmic color was classified as, (1) eosinophilic without keratinization (EOS) (**Figure 3A**), (2) chromophobic (CHR) (**Figure 3A**), (3) basophilic (BAS) (**Figure 3A**), and (4) eosinophilic with keratinization (KRT) (**Figure 3A**). The cytoplasmic internal structure was classified as, (1)

homogenous (HMG) (**Figure 3B**), (2) clear (CLR) (**Figure 3B**), (3) fine granular (FGR) (**Figure 3B**), (4) coarse granular (CGR) (**Figure 3B**), (5) fine vesicular (FVS) (**Figure 3B**), and (6) coarse vesicular (CVS) (**Figure 3B**). Nuclear outline was classified as, (1) smooth (SMT) (**Figure 4A**), (2) grooved (GRV) (**Figure 4A**), and (3) wrinkled (WKL) (**Figure 4A**). A grooved nucleus was one having grooves paralleling the long axis like a coffee bean. Chromatin pattern was defined as, (1) homogenous (HMG) (**Figure 4B**), (2) ground glass (GGL) (**Figure 4B**), (3) fine granular (FGR)

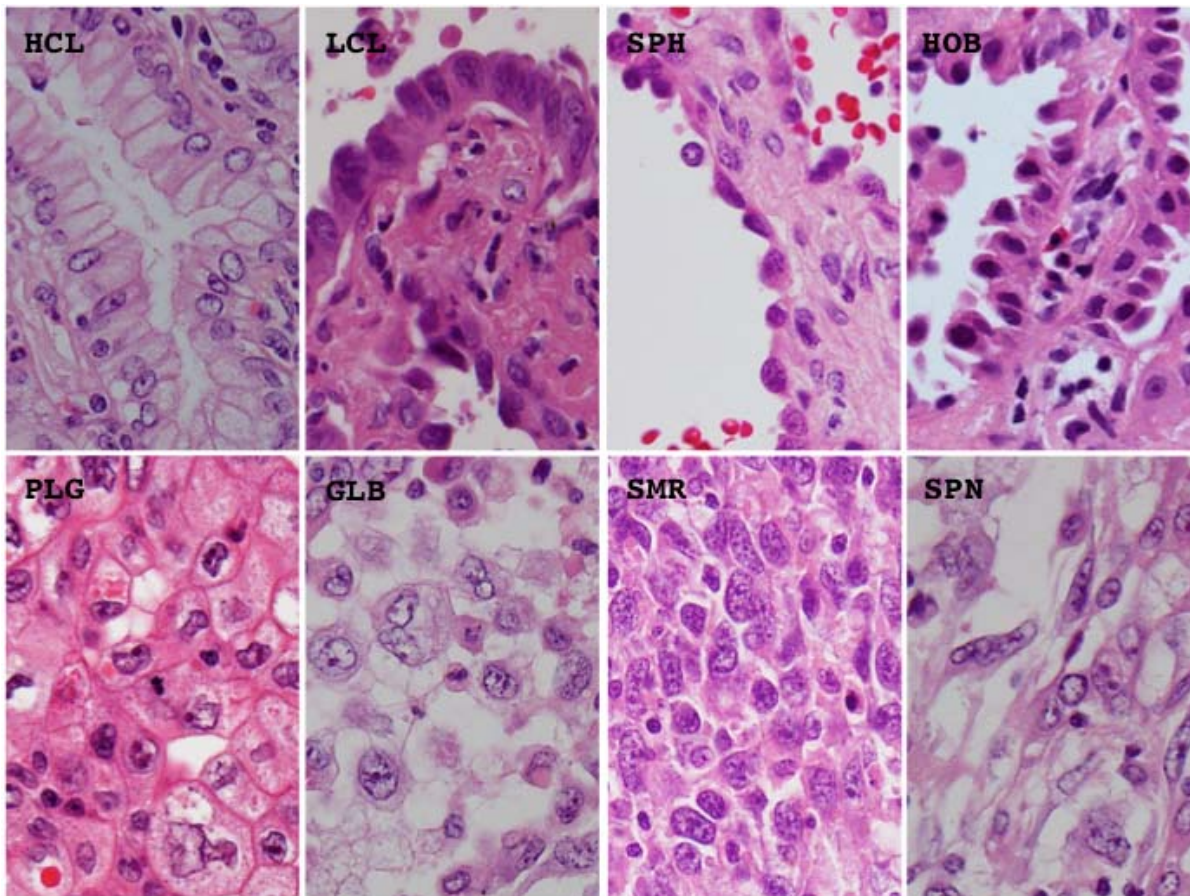


Figure 2. Representative histological appearance of the different cell types. BAC, bronchioloalveolar; HCL, high columnar; LCL, low columnar; SPH, spheroid; HOB, hobnail; PLG, polygonal; GLB, global; SMR, small round; SPN, spindle. Hematoxylin and eosin stain. Magnification is arbitrary.

(**Figure 4B**), (4) coarse granular (CGR) (**Figure 4B**), and (5) clear (CLR) (**Figure 4B**). A fine granular nucleus was one like that observed in non-tumoral bronchiolar epithelial cells. The count of nucleoli was classified as (1) 0 to 1 nucleoli/cell (NL1), (2) 2 to 3 nucleoli/cell (NL2), and (3) 4 or more nucleoli/cell (NL3). The remarkableness of nucleoli was classified as, (1) obscure (NLO) (**Figure 4C**), (2) modest (NLM) (**Figure 4C**), and (3) prominent (NLP) (**Figure 4C**). The largest tumor sections were examined under a light microscope. Proportions as percentages of each pattern were evaluated. Nuclear size, circularity, chromatin density (staining intensity of nucleus), and chromatin granularity (variance of staining intensity of nucleus) were measured in the area where atypical change seemed most prominent in the largest tumor section using NIH image (National Institute of Health, Bethesda, ML). Mean nu-

clear size and mean circularity were calculated from values for at least 50 nuclei. Variations in nuclear size and circularity were determined as variance values. The %mean and %variance of nuclear size, nuclear circularity, chromatin density, and chromatin granularity, were determined as a percentage relative to the maximum value.

Morphometric profiling

Hierarchical clustering (Ward's method) based on the multiple morphometric parameters was performed with computer software (Mulcel, oms-publishing, Saitama, Japan).

Immunohistochemistry

The largest sections of tumors (4 μ m thick) were cut from formalin-fixed, paraffin-embedded tis-

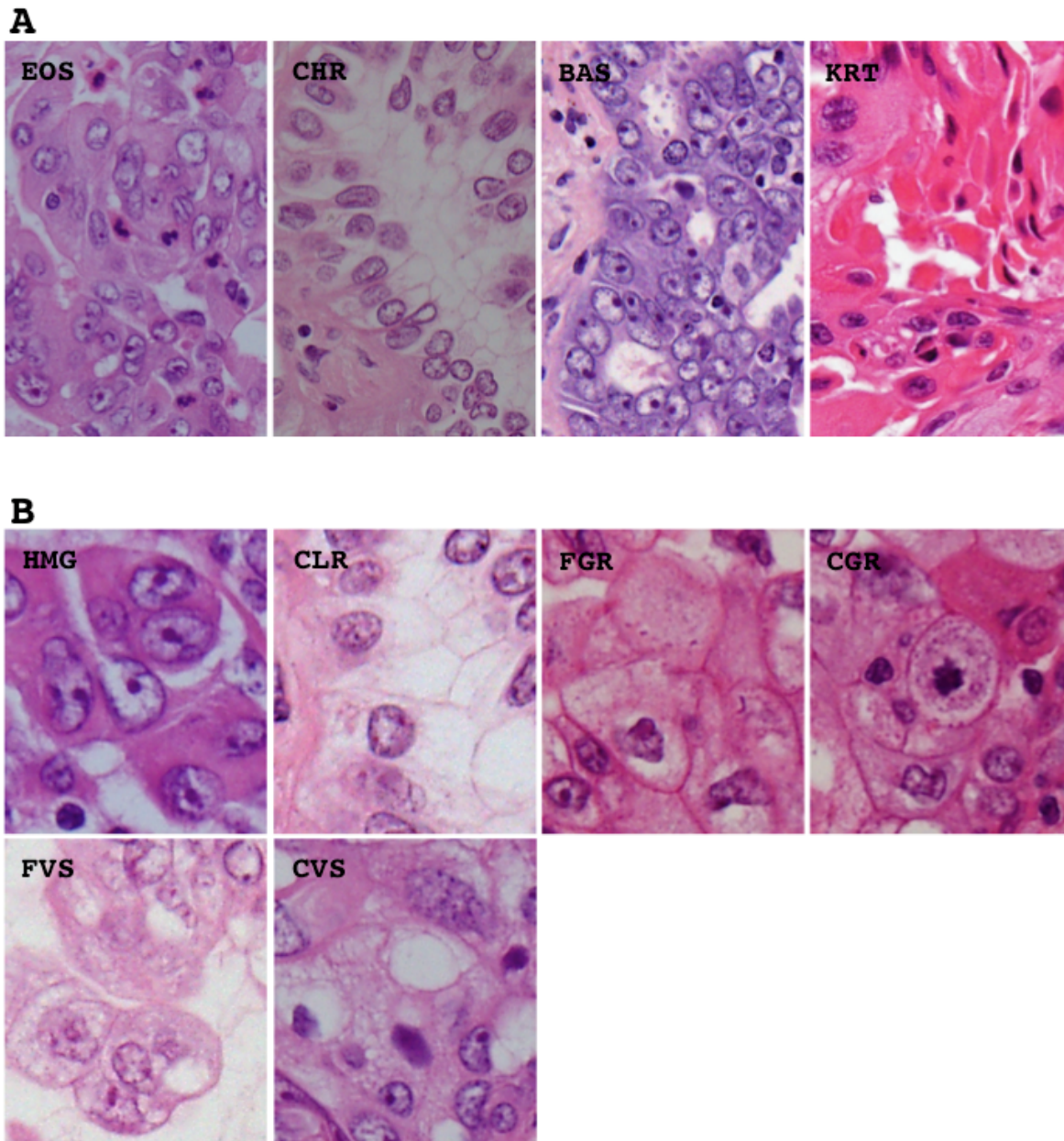


Figure 3. Representative histological appearance of the different cytoplasmic features including color (A) and internal structure (B). EOS, eosinophilic without keratinization; CHR, chromophobic; BAS, basophilic; KRT, eosinophilic with keratinization; HMG, homogenous; CLR, clear; FGR, fine granular; CGR, coarse granular; FVS, fine vesicular; CVS, coarse vesicular. Hematoxylin and eosin stain. Magnification is arbitrary.

sue blocks, and subjected to immunohistochemistry within 48 hours to avoid loss of antigenicity [12,13]. They were deparaffinized, rehydrated, and incubated with 3% hydrogen peroxide, followed by 5% goat serum. The sections

were boiled in citrate buffer (0.01 M, pH 6.0) for 15 minutes to retrieve masked epitopes and then incubated with a primary antibody against Ki-67 (MIB1, DAKO, Ely, UK). Reactivity was visualized using an Envision detection system

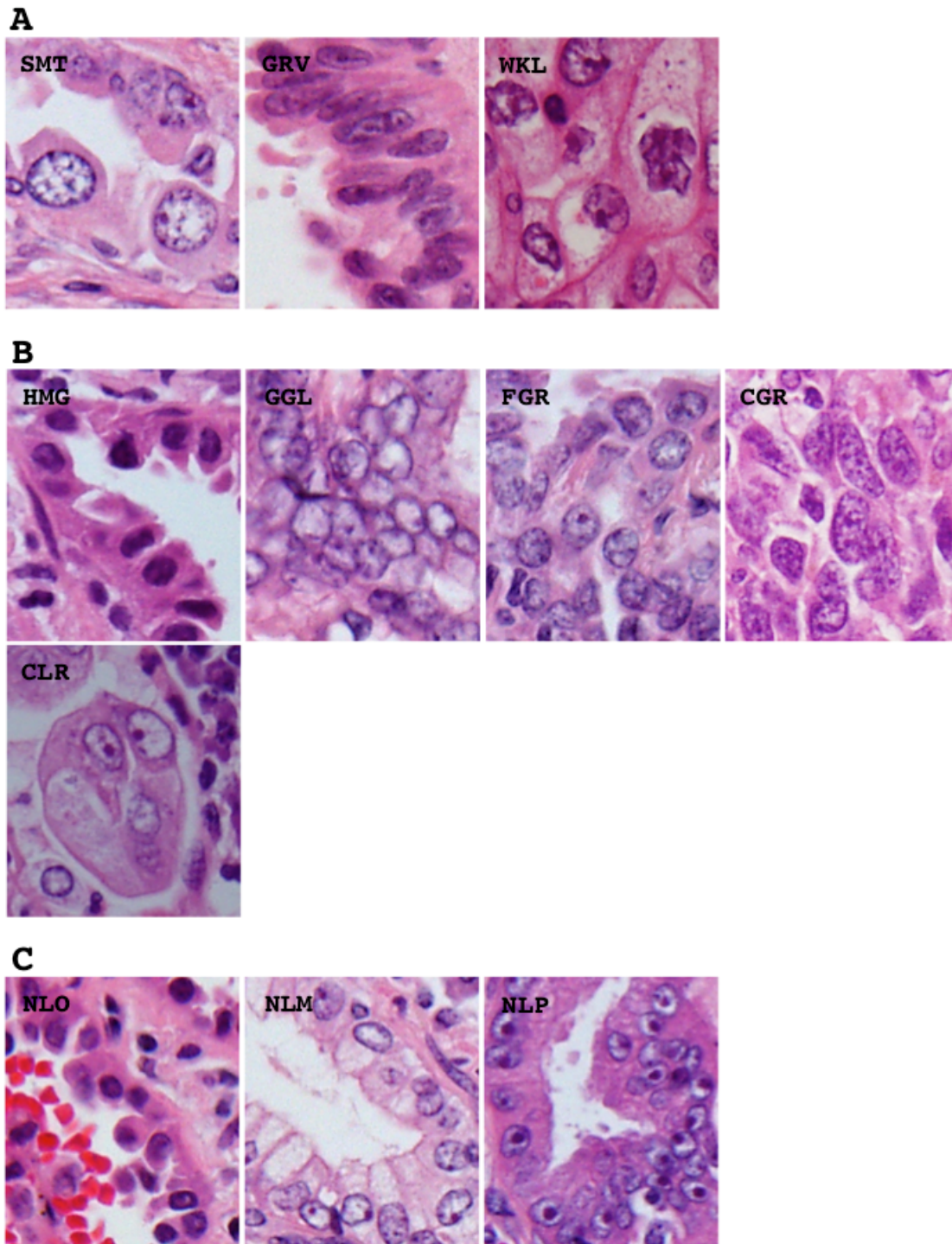
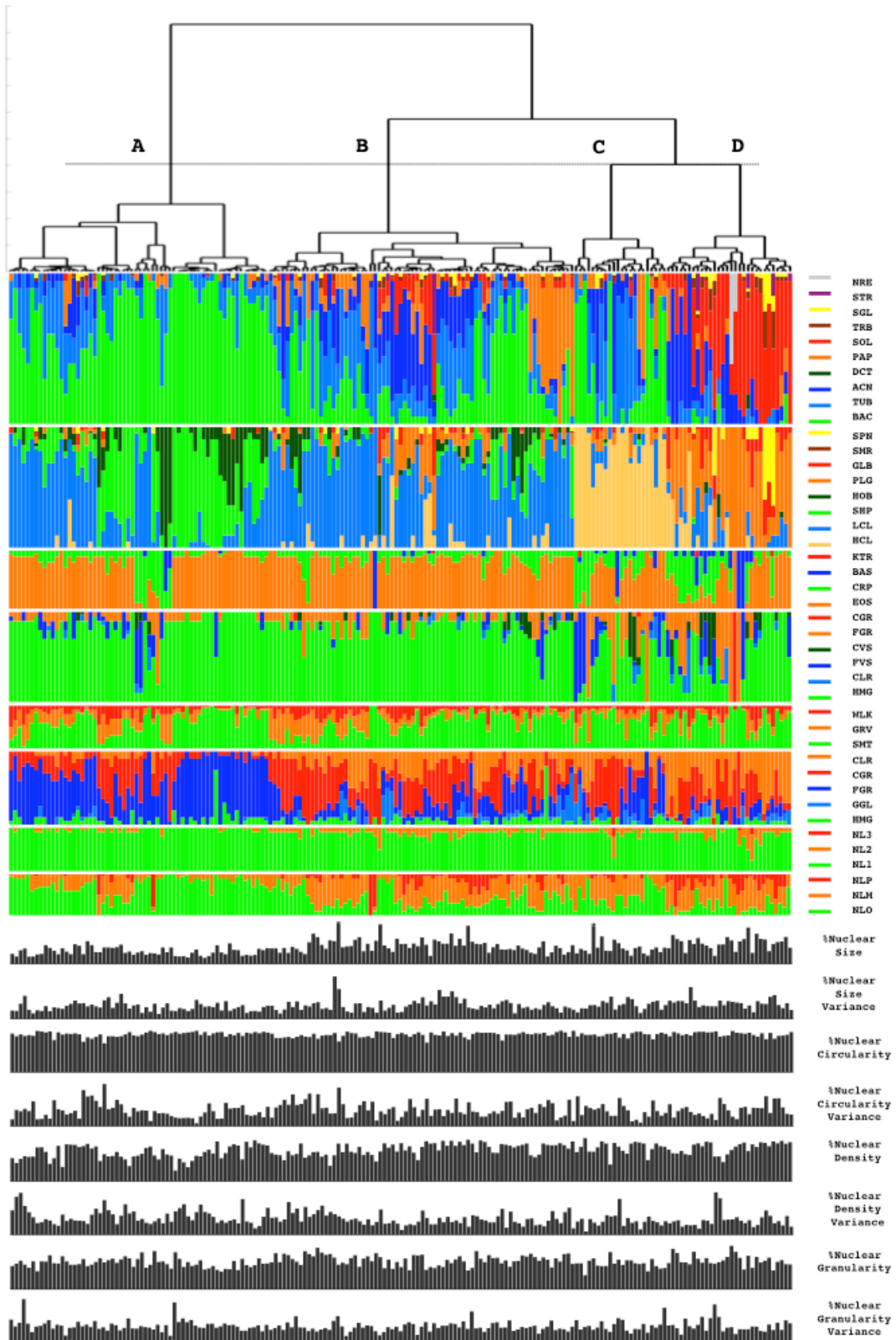


Figure 4. Representative histological appearance of the different nuclear features including nuclear outline (A), chromatin pattern (B) and remarkableness of nucleoli (C). SMT, smooth; GRV, grooved; WKL, wrinkled; HMG, homogeneous; GGL, ground glass; FGR, fine granular; CGR, coarse granular; CLR, clear; NLO, obscure; NLM, modest; NLP, prominent. Hematoxylin and eosin stain. Magnification is arbitrary.

Figure 5 A



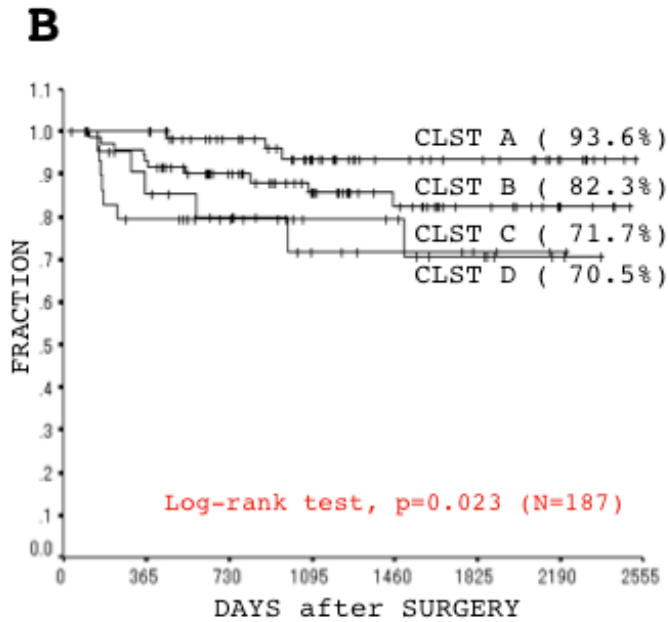


Figure 5. (A, see it in the previous page) Results of hierarchical clustering based on multiple morphological elements in the form of a dendrogram (upper panel). A threshold (upper panel, dashed line) was set to divide lung tumors into four clusters (A to D). Proportions of different patterns for each morphological element among individual tumors are plotted below the dendrogram. The morphological elements analyzed were as follows; histological architecture (second panel: BAC, bronchioloalveolar; TUB, tubular; ACN, acinar; DCT, ductular; TRB, trabecular; PAP, papillary; SOL, solid; SGR, single; SRT, striated; NER, neuroendocrinal), cell type (third panel: HCL, high columnar; LCL, low columnar; SPH, spheroid; HOB, hobnail; PLG, polygonal; GLB, global; SMR, small round; SPN, spindle), cytoplasmic color (fourth panel: EOS, eosinophilic without keratinization; CHR, chromophobic; BAS, basophilic; KRT, eosinophilic with keratinization),

cytoplasmic internal structure (fifth panel: HMG, homogenous; CLR, clear; FGR, fine granular; CGR, coarse granular; FVS, fine vesicular; CVS, coarse vesicular), nuclear outline (sixth panel: SMT, smooth; GRV, groovy; WKL, winkled), chromatin pattern (seventh panel: HMG, homogenous; GGL, ground glass; FGR, fine granular; CGR, coarse granular; CLR, clear), count of nucleoli (eighth panel: NL1, 0 to 1 nucleoli/cell; NL2, 2 to 3 nucleoli/cell; NL3, more nucleoli/cell), remarkableness of nucleoli (ninth panel: NLO, obscure; NLM, modest; NLP, prominent), adjusted (%) nuclear size (tenth panel; maximal value on the Y axis is 100%), adjusted (%) nuclear size variance (eleventh panel; maximal value on the Y axis is 100%), adjusted (%) nuclear circularity (twelfth panel; maximal value on the Y axis is 100%), adjusted (%) nuclear circularity variance (thirteenth panel; maximal value on the Y axis is 100%), adjusted (%) chromatin density (fourteenth panel; maximal value on the Y axis is 100%), adjusted (%) chromatin density variance (fifteenth panel; maximal value on the Y axis is 100%), adjusted (%) chromatin granularity (sixteenth panel; maximal value on the Y axis is 100%), and adjusted (%) chromatin granularity variance (seventeenth panel; maximal value on the Y axis is 100%). (B) Five-year disease-free survival curves evaluated from a Kaplan-Meier analysis among the morphometric clusters. CLST means cluster. Values in parentheses are estimated five-year disease-free survival rates.

(DAKO), and the nuclei were counterstained with hematoxylin. A Ki-67 labeling index (MIB1 index) was calculated as a proportion of positive cells by counting 500 or more neoplastic cells in an area where the immunolabeling seemed representative.

Statistical analysis

Disease-free survival curves were plotted using the Kaplan-Meier method, and used to estimate the absolute risk of recurrence at five years. Differences in the disease-free survival (DFS) span and rate were analyzed using the log-rank test. Differences in metric factors among the morphometric clusters were analyzed with Stu-

dent's t test. Associations between the clusters and clinicopathologic features and genetic mutations were analyzed with Fisher's exact test. P values less than 0.0500 were considered significant. All the statistical analyses were performed using SPSS software (SPSS for Windows Version 10.0; SPSS; Chicago, IL).

Results

Essential morphometric elements to predict outcome

Hierarchical clustering of whole morphometric parameters was used to evaluate similarities among the tumors and to draw a dendrogram

Figure 6-1

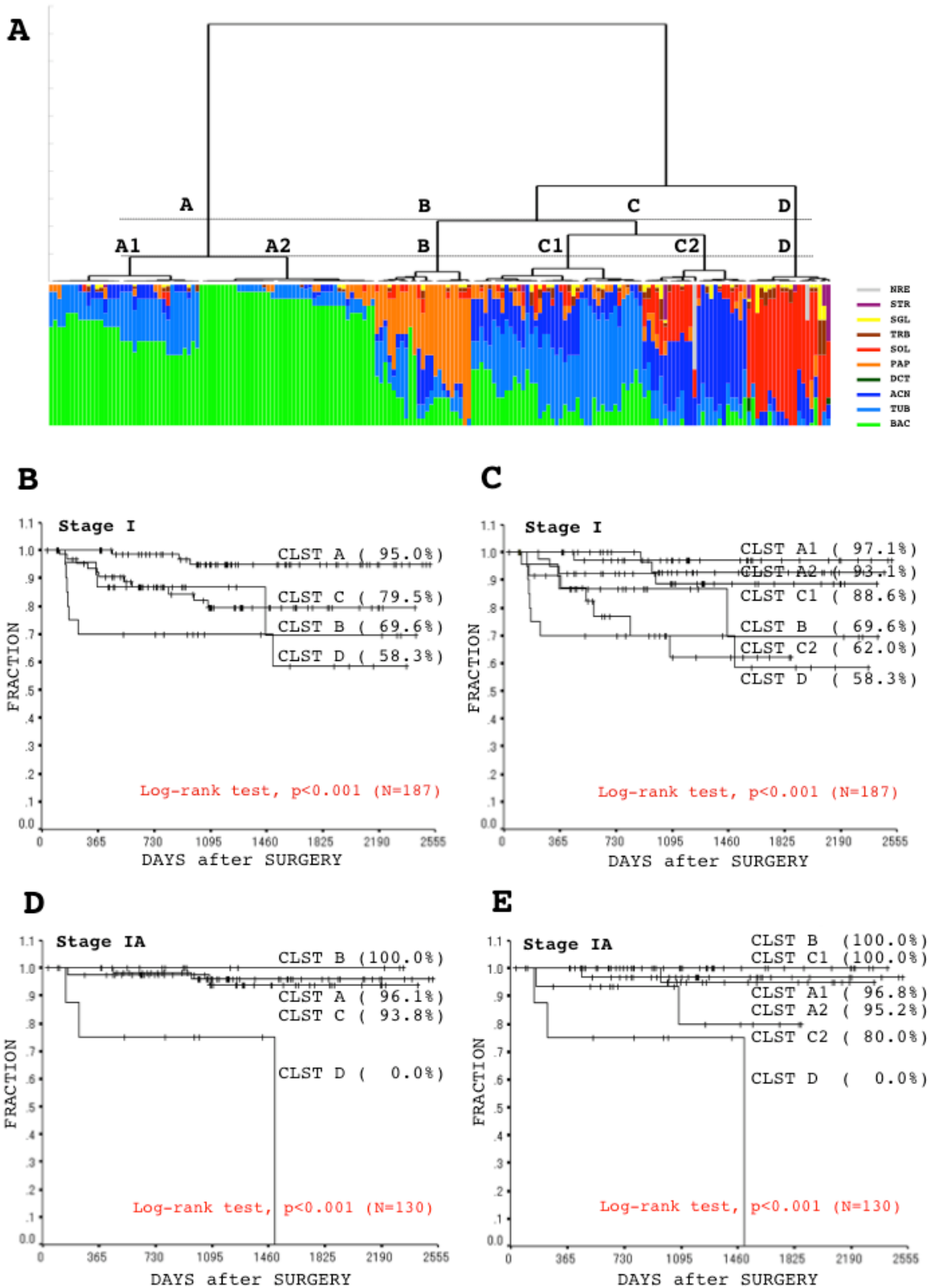


Figure 6-2

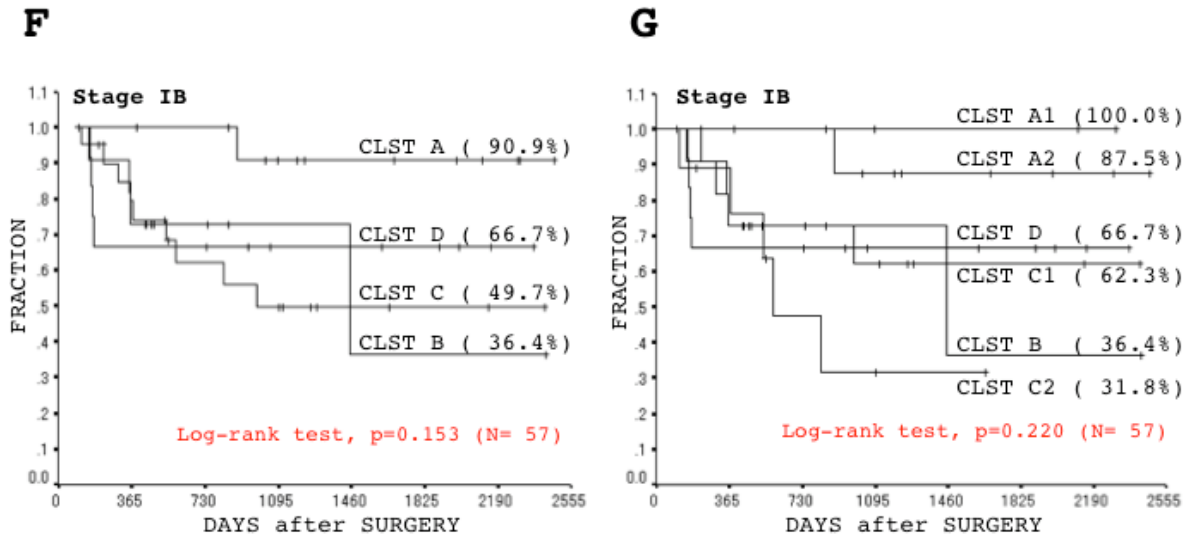


Figure 6. (see A-D in previous page) (A) Results of hierarchical clustering based on an element of histological architecture in the form of a dendrogram (upper panel). A threshold (upper panel, dashed lines) was set to divide lung tumors into four clusters (A to D) and six sub-clusters (A1, A2, B, C1, C2, and D). Proportions of different architectural elements among individual tumors are plotted below the dendrogram (lower panel: BAC, bronchioalveolar; TUB, tubular; ACN, acinar; DCT, ductular; TRB, trabecular; PAP, papillary; SOL, solid; SGR, single; SRT, striated; NER, neuroendocrinal). (B to G) Five-year disease-free survival curves evaluated from a Kaplan-Meier analysis among the architectural clusters (stage I whole (B), stage IA (D), stage IB (F)) and sub-clusters (stage I whole (C), stage IA (E), stage IB (G)). CLST means cluster. Values in parentheses are estimated five-year disease-free survival rates.

(Figure 5A). We tentatively set a threshold (Figure 5A, dashed line) to divide the cases into four clusters (Figure 5, cluster A to D), because a number around five was considered convenient for a screening analysis. The results confirmed potential prognostic value of the subtyping system based on morphometric profiling, as the estimated disease-free survival significantly differed among the four clusters (Figure 5B). To identify essential morphologic elements having prognostic value, possible associations between individual (or combination of) elements and postoperative outcome were analyzed. Tumors among clusters based on architectural element (ARC-CLSTs) showed the most significant difference in the crude recurrence rate and estimated disease-free survival, and the highest recurrence risk (hazard ratio) (Figure 6 and Table 1). (Dendrograms drawn from parameters of cellular features [cell type + cytoplasmic color + cytoplasmic internal structure] (CLL-CLST), nuclear features [nuclear outline + chromatin pattern + nucleoli count + nucleoli remarkableness + nuclear size + nuclear size variance + nuclear

circularity + chromatin density + chromatin density variance + chromatin granularity + chromatin granularity variance] (NCL-CLST), a combination of architectural and cellular features (ARC+CLL-CLST), a combination of cellular and nuclear features (CLL+NCL-CLST), and a combination of architectural and nuclear features (ARC+NCL-CLST), are not shown. If readers request presentation of the data, the authors will provide as occasion demands.). The findings suggested histological architecture to be the most important, and an essential element for predicting postoperative outcome. Therefore, we focused on the ARC-CLSTs and further subdivided the clusters (Figure 6A). Significant differences in the estimated disease-free survival, crude recurrence ratio, and hazard rate were observed also among the six sub-clusters (Figure 6A [A1, A2, B, C1, C2, and D] and 6C, Table 2). Moreover, the sub-clusters provided an advantage over the original four clusters when it came to separating tumors, especially those with a better outcome (Figure 6A and 6C, Table 3). Similar findings were obtained when

Improved histological subtyping of lung adenocarcinoma

Table 1. Recurrence rates and hazard ratios among clusters based on different elements

	Crude recurrence rate % [No.]	Hazard ratio [95% CI]
WHL	P = 0.177	
CLST A [61]	4.9 [3]	1.00 [ref.]
B [73]	13.7 [10]	2.97 [0.82-10.79]
C [22]	22.7 [5]	5.59 [1.33-23.41]
D [31]	22.6 [7]	5.85 [1.51-22.66]
ARC	P = 0.012	
CLST A [73]	3.9 [3]	1.00 [ref.]
B [23]	17.4 [4]	5.53 [1.23-24.77]
C [67]	16.4 [11]	4.90 [1.37-17.57]
D [20]	35.0 [7]	11.34 [2.93-43.88]
CLL	P = 0.153	
CLST A [84]	11.9 [10]	1.00 [ref.]
B [30]	3.3 [1]	0.27 [0.04- 2.13]
C [36]	25.0 [9]	2.57 [1.04- 6.33]
D [37]	13.5 [5]	1.34 [0.46- 3.92]
NCL	P = 0.260	
CLST A [43]	7.0 [3]	1.00 [ref.]
B [48]	18.8 [9]	2.94 [0.80-10.85]
C [58]	10.3 [6]	1.51 [0.38- 6.03]
D [38]	18.4 [7]	3.20 [0.83-12.39]
CLL-NCL	P = 0.642	
CLST A [46]	10.9 [5]	1.00 [ref.]
B [29]	6.9 [2]	0.66 [0.13- 3.38]
C [29]	13.8 [4]	1.53 [0.41- 5.71]
D [83]	16.9 [14]	1.66 [0.60- 4.61]
ARC-CLL	P = 0.138	
CLST A [54]	3.7 [2]	1.00 [ref.]
B [70]	15.7 [11]	4.43 [0.98-19.98]
C [31]	16.1 [5]	4.65 [0.90-23.99]
D [32]	21.9 [7]	7.53 [1.56-36.28]
ARC-NCL	P = 0.044	
CLST A [66]	6.1 [4]	1.00 [ref.]
B [26]	3.8 [1]	0.65 [0.07- 5.77]
C [76]	19.7 [15]	3.88 [1.29-11.69]
D [19]	26.3 [5]	6.10 [1.63-22.80]

No., number of cases; P, P value, calculated with Fisher's exact test; CI, confidence interval; ref., reference; CLST, cluster; WHL, whole elements; ARC, architectural element; CLL, cell type and cytoplasmic elements; NCL, nuclear element.

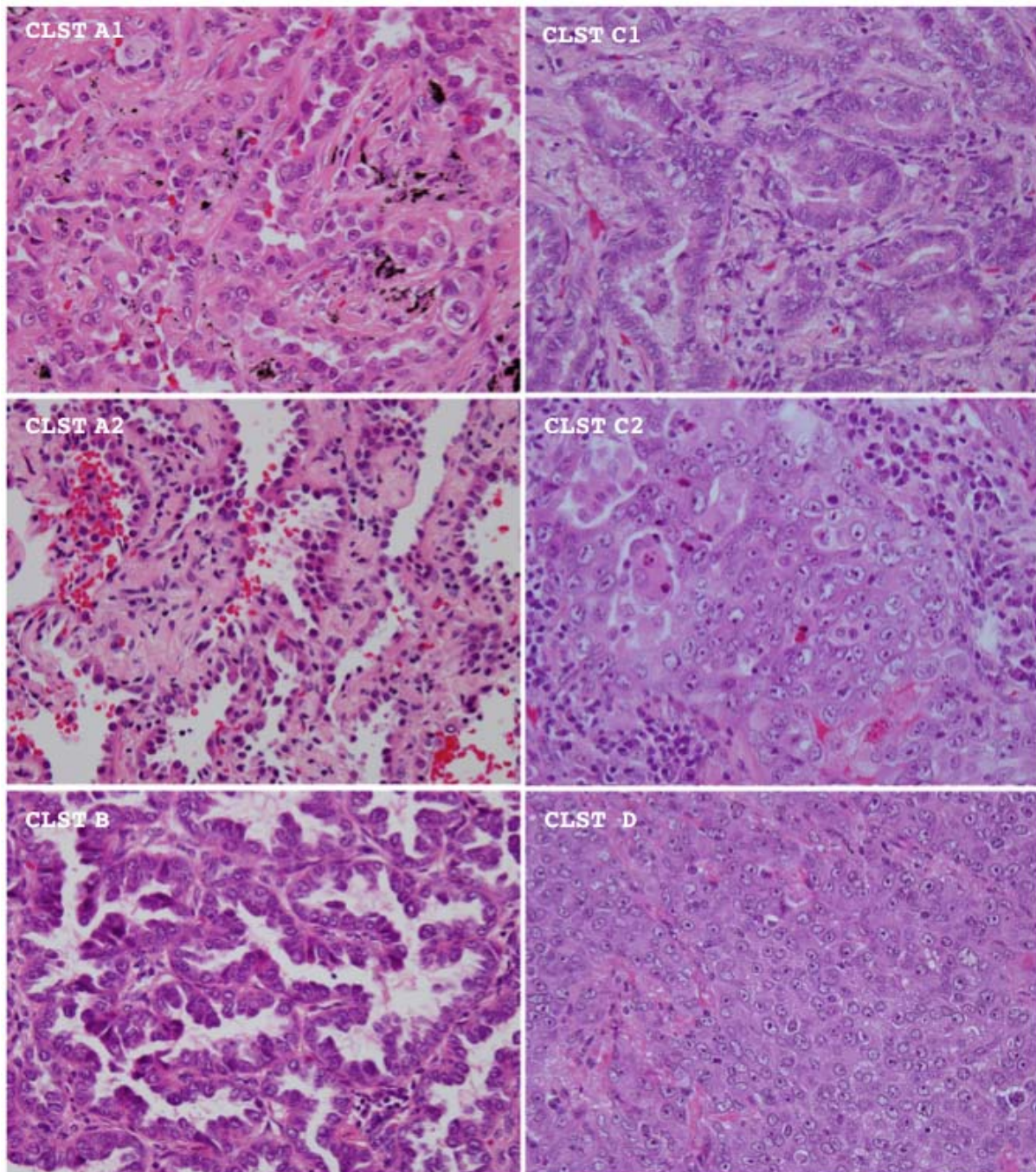


Figure 7. The representative histological appearance of tumors among different architectural sub-clusters is shown. Hematoxylin and eosin stain. CLST means cluster. Magnification is $\times 400$.

restricted in stage IA, but not stage IB, disease (Figure 6C, 6D, 6E and 6F, Table 2, and Table 3). Either tumor size or pleural invasion (determinants of stage IB disease) is very important in determining outcome [2,11]. The consid-

erable influence of such factors can be a one of explanations why there was no association between the sub-clusters and outcome among stage IB disease.

Improved histological subtyping of lung adenocarcinoma

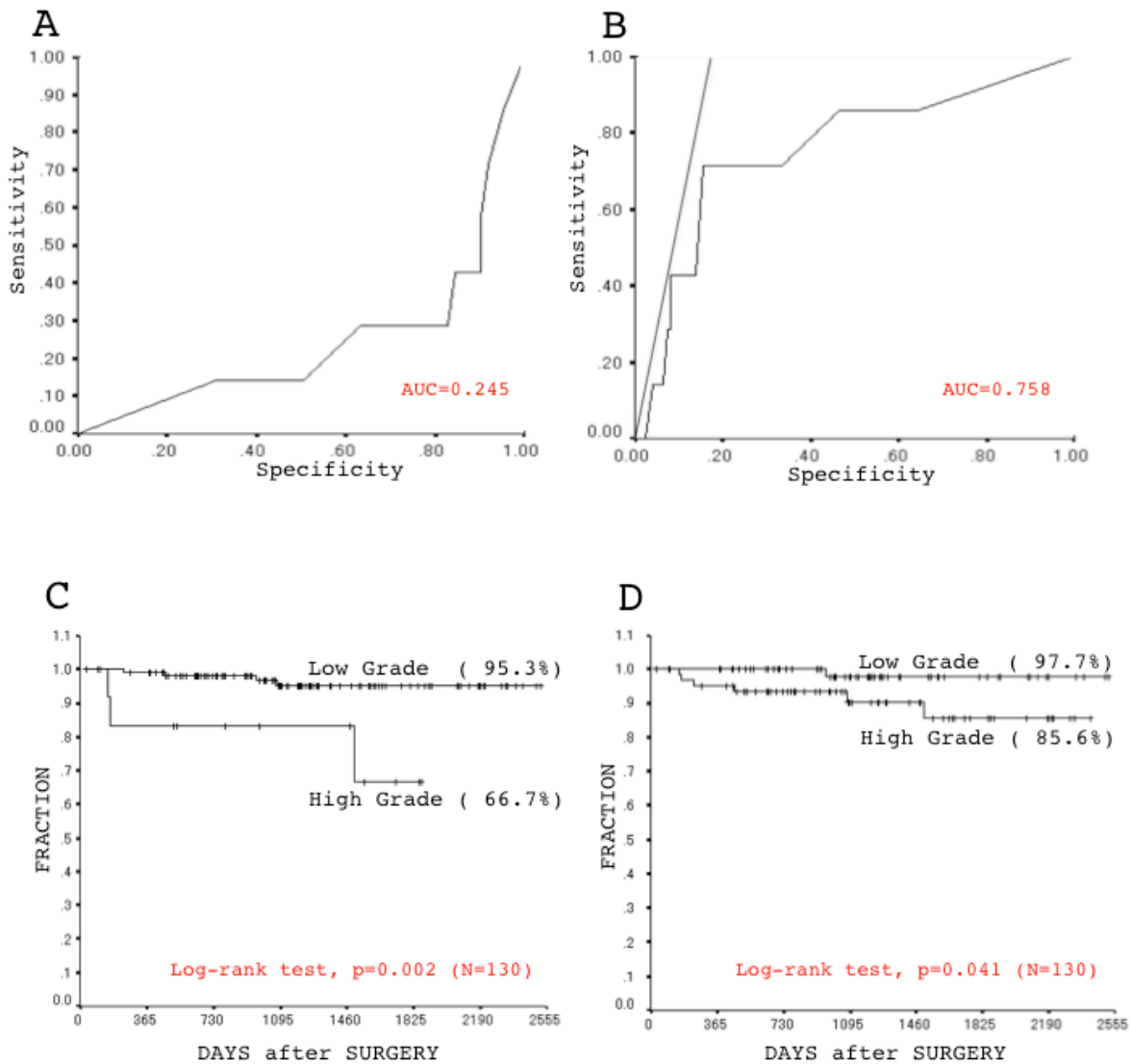


Figure 8. The relative operating characteristic (ROC) curve was described based on the proportion of either low-grade (A) or high-grade (B) components among tumors of stage IA ADC. AUC is the area under the curve (AUC). Five-year disease-free survival curves was evaluated based on a Kaplan-Meier analysis of the sub-groups according to a cut-off value of 72.0% (C) and of 9.0% (D) in a proportion of the high-grade component among stage IA disease. Values in parentheses are estimated five-year disease-free survival rates.

Pathologic features among the sub-clusters

Tumors tended to be larger in sub-cluster D (**Table 4**). Pleural invasion occurred among tumors of all the sub-clusters except A1, and tended to be severe among tumors of sub-clusters B, C1, C2, and D (**Table 4**). Lymphatic canal and vascular involvement was observed for tumors of all sub-clusters, but tended to more frequent among tumors of sub-clusters

C1, C2, and D (**Table 4**). Growth activity measured by Ki-67 immunolabeling (the MIB1 index) tended to be stronger in sub-clusters C2, and D. These findings were well consistent with postoperative outcome among the sub-clusters (**Figure 6** and **Table 3**).

Personal features among the sub-clusters

No difference in age of onset was found among

Improved histological subtyping of lung adenocarcinoma

Table 2. Postoperative recurrence rates and hazard ratios in ARC-CLSTs among sub-stages

	Crude recurrence rate % [No.]	Hazard ratio [95% CI]
Stage I	P = 0.002	P < 0.001
CLST A [78]	3.8 [3]	1.00 [ref.]
B [23]	17.4 [4]	5.59 [1.25- 25.06]
C [66]	16.7 [11]	4.96 [1.38- 17.78]
D [20]	35.0 [7]	11.47 [2.96- 44.39]
Stage IA	P = 0.007	P < 0.001
CLST A [65]	3.1 [2]	1.00 [ref.]
B [12]	0.0 [0]	N.A.
C [45]	4.4 [2]	1.53 [0.22- 10.89]
D [8]	37.5 [3]	17.18 [2.82-104.69]
Stage IB	P = 0.191	P = 0.153
CLST A [13]	7.7 [1]	1.00 [ref.]
B [11]	36.4 [4]	7.45 [0.82- 67.44]
C [21]	42.9 [9]	7.82 [0.99- 61.94]
D [12]	33.3 [4]	5.77 [0.64- 51.67]

ARC-CLSTs, clusters based on architectural elements; No., number of cases; CLST, cluster; P, P value for crude recurrence rate and hazard ratio are calculated by Fisher's exact test and Log-rank test, respectively; CI, confidence interval; ref., reference; N.A., not available. Squamous cell carcinomas were excluded from analysis.

Table 3. Postoperative recurrence rates and hazard ratios in ARC-subCLSTs among sub-stages

	Crude recurrence rate % [No.]	Hazard ratio [95% CI]
Stage I	P = 0.002	P < 0.001
CLST A1 [36]	2.8 [1]	1.00 [ref.]
A2 [42]	4.8 [2]	1.84 [0.17- 20.26]
B [23]	17.4 [4]	8.07 [0.90- 72.41]
C1 [41]	9.8 [4]	3.90 [0.44- 34.92]
C2 [25]	28.0 [7]	13.51 [1.66-109.98]
D [20]	35.0 [7]	16.49 [2.03-134.14]
Stage IA	P = 0.003	P < 0.001
CLST A1 [32]	3.1 [1]	1.00 [ref.]
A2 [33]	3.0 [1]	1.14 [0.07- 18.30]
B [12]	0.0 [0]	N.A.
C1 [29]	0.0 [0]	N.A.
C2 [16]	12.5 [2]	5.14 [0.47- 56.86]
D [8]	37.5 [3]	18.44 [1.88-181.10]
Stage IB	P = 0.310	P = 0.220
CLST A1 [4]	0.0 [0]	1.00 [ref.]
A2 [9]	11.1 [1]	N.A.
B [11]	36.4 [4]	N.A.
C1 [12]	33.3 [4]	N.A.
C2 [9]	55.6 [5]	N.A.
D [12]	33.3 [4]	N.A.

ARC-subCLSTs, sub-clusters based on architectural elements; No., number of cases; CLST, cluster; P, P value for crude recurrence rate and hazard ratio are calculated by Fisher's exact test and Log-rank test, respectively; CI, confidence interval; ref., reference; N.A., not available; *C3 (squamous cell carcinomas), excluded from analysis.

Improved histological subtyping of lung adenocarcinoma

Table 4. Association between ARC-subCLST and pathobiological features

Cluster	A1	A2	B	C1	C2	D
Stage I [191]	[36]	[42]	[23]	[41]	[25]	[20]
Size [mean ± SD mm] [24.8 ± 16.7 (7.0 to 120.0)] (<i>Student's t test, p < 0.0100: [A1,A2] vs [D]</i>)	19.3 ± 7.6	21.6 ± 13.8	26.4 ± 15.1	26.5 ± 19.2	26.7 ± 17.7	35.2 ± 23.5
Pleural invasion (Fisher's exact test, p = 0.0002)						
0 [158]	36 [100.0%]	41 [97.6%]	17 [74.0%]	29 [70.7%]	18 [72.0%]	14 [70.0%]
1 [23]	0 [0.0%]	1 [2.4%]	3 [13.0%]	9 [22.0%]	7 [28.0%]	2 [10.0%]
2 [10]	0 [0.0%]	0 [0.0%]	3 [13.0%]	3 [7.3%]	0 [0.0%]	4 [20.0%]
Lymphatic canal involvement (Fisher's exact test, p < 0.0001)						
0 [61]	12 [33.3%]	31 [73.8%]	8 [34.8%]	6 [14.6%]	2 [8.0%]	2 [10.0%]
1 [110]	23 [63.9%]	11 [26.2%]	13 [56.5%]	31 [75.6%]	19 [76.0%]	11 [55.0%]
2 [18]	1 [2.8%]	0 [0.0%]	2 [8.7%]	4 [9.8%]	4 [16.0%]	5 [25.0%]
3 [2]	0 [0.0%]	0 [0.0%]	0 [0.0%]	0 [0.0%]	0 [0.0%]	2 [10.0%]
Vascular involvement (Fisher's exact test, p < 0.0001)						
0 [129]	29 [80.6%]	41 [97.6%]	13 [56.5%]	28 [68.3%]	10 [40.0%]	6 [30.0%]
1 [46]	6 [16.7%]	0 [0.0%]	8 [34.8%]	12 [29.3%]	11 [44.4%]	7 [35.0%]
2 [14]	1 [2.7%]	1 [2.4%]	2 [8.7%]	1 [2.4%]	4 [16.0%]	5 [25.0%]
3 [2]	0 [0.0%]	0 [0.0%]	0 [0.0%]	0 [0.0%]	0 [0.0%]	2 [10.0%]
Grwth activity [MIB1 index, mean ± SD %] [15.4 ± 17.5 (0.1 to 80.7)] (<i>Student's t test, p < 0.0001: [A1,A2] vs [C2,D]</i>)	7.6 ± 12.7	4.4 ± 8.7	11.8 ± 13.0	15.1 ± 13.2	31.2 ± 21.1	33.5 ± 15.8
Stage IA [133]	[32]	[33]	[12]	[29]	[16]	[8]
Size [mean ± SD mm] [19.3 ± 7.6 (7.0 to 30.0)] (<i>Student's t test, no significant difference</i>)	18.0 ± 6.7	15.7 ± 6.8	16.7 ± 7.7	18.0 ± 6.2	16.8 ± 4.9	14.8 ± 5.6
Pleural invasion (Fisher's exact test, p = 0.0188)						
0 [122]	32 [100.0%]	33 [100.0%]	10 [83.3%]	24 [82.8%]	13 [81.3%]	8 [100.0%]
1 [11]	0 [0.0%]	0 [0.0%]	2 [16.7%]	5 [17.2%]	3 [18.7%]	0 [0.0%]
Lymphatic canal involvement (Fisher's exact test, p < 0.0001)						
0 [52]	11 [34.4%]	28 [84.8%]	5 [36.4%]	5 [17.2%]	2 [12.5%]	1 [12.5%]
1 [74]	21 [65.6%]	5 [15.2%]	7 [63.6%]	23 [79.4%]	12 [75.0%]	4 [50.0%]
2 [6]	0 [0.0%]	0 [0.0%]	0 [0.0%]	1 [3.4%]	2 [12.5%]	2 [25.0%]
3 [1]	0 [0.0%]	0 [0.0%]	0 [0.0%]	0 [0.0%]	0 [0.0%]	1 [12.5%]
Vascular involvement (Fisher's exact test, not suitable for analysis)						
0 [99]	26 [81.3%]	33 [100.0%]	7 [58.3%]	22 [75.9%]	7 [43.8%]	3 [37.5%]
1 [29]	6 [18.7%]	0 [0.0%]	4 [33.3%]	7 [24.1%]	8 [50.0%]	2 [25.0%]
2 [5]	0 [0.0%]	0 [0.0%]	1 [8.4%]	0 [0.0%]	1 [6.3%]	3 [37.5%]
3 [0]	0 [0.0%]	0 [0.0%]	0 [0.0%]	0 [0.0%]	0 [0.0%]	0 [0.0%]
Growth activity [MIB1 index, mean ± SD %] [12.4 ± 15.4 (0 to 66.1)] (<i>Student's t test, p < 0.0010: [A1,A2] vs [C2,D]</i>)	7.2 ± 13.4	4.4 ± 9.7	9.1 ± 14.3	13.0 ± 12.1	26.3 ± 14.8	27.5 ± 13.6
Stage IB [58]	[4]	[9]	[11]	[12]	[9]	[12]
Size [mean ± SD mm] [43.2 ± 18.5 (10.0 to 120.0)] (<i>Student's t test, no significant difference</i>)	30.0 ± 6.8	40.5 ± 13.7	35.1 ± 15.0	47.0 ± 27.0	44.4 ± 18.5	48.9 ± 20.5
Pleural invasion (Fisher's exact test, p = 0.1715)						
0 [34]	4 [100.0%]	5 [55.6%]	8 [72.7%]	5 [41.7%]	5 [55.6%]	6 [50.0%]
1 [15]	0 [0.0%]	4 [44.4%]	1 [9.1%]	4 [33.3%]	4 [44.4%]	2 [16.7%]
2 [9]	0 [0.0%]	0 [0.0%]	2 [18.2%]	3 [25.0%]	0 [0.0%]	4 [33.3%]
Lymphatic canal involvement (Fisher's exact test, p = 0.5434)						
0 [11]	1 [25.0%]	4 [44.4%]	3 [27.3%]	1 [8.3%]	0 [0.0%]	1 [8.3%]
1 [35]	2 [50.0%]	5 [55.6%]	6 [54.5%]	8 [66.7%]	7 [77.8%]	7 [58.4%]
2 [11]	1 [25.0%]	0 [0.0%]	2 [18.2%]	3 [25.0%]	2 [22.2%]	3 [25.0%]
3 [1]	0 [0.0%]	0 [0.0%]	0 [0.0%]	0 [0.0%]	0 [0.0%]	1 [8.3%]
Vascular involvement (Fisher's exact test, p = 0.0547)						
0 [31]	3 [75.0%]	9 [100.0%]	6 [54.5%]	6 [50.0%]	3 [33.3%]	3 [25.0%]
1 [17]	0 [0.0%]	0 [0.0%]	4 [36.4%]	5 [41.7%]	3 [33.3%]	5 [41.6%]
2 [8]	1 [25.0%]	0 [0.0%]	1 [9.1%]	1 [8.3%]	3 [33.3%]	2 [16.7%]
3 [2]	0 [0.0%]	0 [0.0%]	0 [0.0%]	0 [0.0%]	0 [0.0%]	2 [16.7%]
Growth activity [MIB1 index, mean ± SD %] [20.1 ± 26.0 (0.1 to 80.7)] (<i>Student's t test, p < 0.0100: [A1,A2] vs [D]</i>)	10.8 ± 5.1	4.5 ± 4.2	14.3 ± 11.7	20.0 ± 14.8	39.7 ± 28.2	37.5 ± 16.4

ARC-subCLST, sub-clusters based on architectural element; SD, standard deviation; NA, not available.

Improved histological subtyping of lung adenocarcinoma

Table 5. Association between ARC-subCLST and personal characteristics

Cluster	A1	A2	B	C1	C2	D
Stage I [191]	[36]	[42]	[23]	[41]	[25]	[20]
Age [mean ± SD Y/O] [67.8 ± 8.3 (45 to 85)] (<i>Student's t test, no significant difference</i>)	69.2 ± 7.6	66.0 ± 8.0	66.7 ± 10.3	68.2 ± 8.4	69.9 ± 8.4	66.8 ± 8.1
Sex (Fisher's exact test, p = 0.0967)						
Female [91]	20 [55.6%]	25 [59.5%]	11 [47.8%]	20 [48.8%]	6 [24.0%]	8 [40.0%]
Male [100]	16 [44.4%]	17 [40.5%]	12 [52.2%]	21 [51.2%]	19 [76.0%]	12 [60.0%]
Smoking History						
Status (Fisher's exact test, p = 0.0012)						
None [96]	27 [75.0%]	28 [66.7%]	12 [52.2%]	16 [40.0%]	7 [29.2%]	6 [33.3%]
Smoker [91]	9 [25.0%]	14 [33.3%]	11 [47.8%]	24 [60.0%]	17 [70.8%]	12 [66.7%]
N.A. [4]	0 [-]	0 [-]	0 [-]	1 [-]	1 [-]	2 [-]
Brinkmann index [mean ± SD] [454 ± 593 (0 to 3200)] (<i>Student's t test, P < 0.0500: [A1,A2] vs [C2,D]</i>)	184 ± 333	316 ± 564	560 ± 708	479 ± 604	743 ± 586	682 ± 705
Stage IA [133]	[32]	[33]	[12]	[29]	[16]	[8]
Age [mean ± SD Y/O] [67.8 ± 7.7 (51 to 85)] (<i>Student's t test, no significant difference</i>)	69.3 ± 7.1	66.5 ± 7.3	66.5 ± 8.8	68.2 ± 8.4	69.3 ± 7.6	70.0 ± 6.1
Sex (Fisher's exact test, p = 0.0356)						
Female [66]	18 [56.2%]	21 [65.6%]	6 [45.5%]	16 [55.2%]	4 [25.0%]	1 [12.5%]
Male [67]	14 [43.8%]	12 [34.4%]	6 [54.5%]	13 [44.8%]	12 [75.0%]	7 [87.5%]
Smoking History						
Status (Fisher's exact test, p = 0.0067)						
None [71]	24 [75.0%]	23 [69.6%]	5 [41.7%]	12 [41.4%]	5 [33.3%]	2 [28.6%]
Smoker [60]	8 [25.0%]	10 [30.4%]	7 [58.3%]	17 [58.6%]	10 [66.7%]	5 [71.4%]
N.A. [2]	0 [-]	0 [-]	0 [-]	0 [-]	1 [-]	1 [-]
Brinkmann index [mean ± SD] [413 ± 574 (0 to 3200)] (<i>Student's t test, P < 0.0500: [A1,A2] vs [C2,D]</i>)	186 ± 339	247 ± 436	670 ± 708	473 ± 665	732 ± 650	758 ± 754
Stage IB [58]	[4]	[9]	[11]	[12]	[9]	[12]
Age [mean ± SD Y/O] [67.9 ± 9.8 (45 to 84)] (<i>Student's t test, no significant difference</i>)	68.0 ± 12.4	64.4 ± 10.1	66.8 ± 11.2	72.4 ± 6.8	71.3 ± 10.1	64.7 ± 8.7
Sex (Fisher's exact test, p = 0.8977)						
Female [21]	2 [50.0%]	3 [33.3%]	5 [54.5%]	4 [33.3%]	2 [22.2%]	4 [33.3%]
Male [37]	2 [50.0%]	6 [66.7%]	6 [45.5%]	8 [66.7%]	7 [77.8%]	8 [66.7%]
Smoking History						
Status (Fisher's exact test, p = 0.3097)						
None [27]	3 [75.0%]	6 [66.7%]	8 [72.7%]	4 [36.4%]	2 [22.2%]	4 [36.4%]
Smoker [29]	1 [25.0%]	3 [33.3%]	3 [27.3%]	7 [63.6%]	7 [77.8%]	7 [63.6%]
N.A. [2]	0 [-]	0 [-]	0 [-]	1 [-]	0 [-]	1 [-]
Brinkmann index [mean ± SD] [544 ± 629 (0 to 2500)] (<i>Student's t test, no significant difference</i>)	165 ± 330	531 ± 845	459 ± 723	496 ± 426	763 ± 496	734 ± 706

ARC-subCLST, sub-clusters based on architectural element; SD, standard deviation; Y/O, year-old; None, non-smoker; N.A., not available.

Improved histological subtyping of lung adenocarcinoma

Table 6. Proportions of different elements among ARC-subCLSTs in stage IA disease

Cluster	A1 [32]	A2 [33]	B [12]	C1 [29]	C2 [16]	D [8]
BAC	64.9 ± 9.8	90.9 ± 7.1	22.3 ± 16.1	22.4 ± 13.1	4.7 ± 6.2	2.8 ± 7.0
TUB	27.7 ± 9.8	6.0 ± 4.5	16.8 ± 12.5	49.1 ± 17.9	11.3 ± 7.9	3.7 ± 5.2
ACI	4.7 ± 4.2	0.7 ± 1.7	8.6 ± 13.6	19.1 ± 11.0	55.0 ± 19.9	6.2 ± 10.6
DCT	0.0 ± 0.0	0.0 ± 0.0	0.0 ± 0.0	0.0 ± 0.0	0.0 ± 0.0	1.3 ± 3.5
PAP	1.3 ± 2.8	2.0 ± 3.9	50.9 ± 22.1	5.2 ± 4.5	5.3 ± 7.2	2.5 ± 7.0
SOL	0.5 ± 2.0	0.0 ± 0.0	2.3 ± 3.4	1.8 ± 3.8	17.2 ± 14.0	70.3 ± 14.8
TRB	0.7 ± 1.5	0.3 ± 0.8	0.3 ± 0.9	1.6 ± 2.5	0.9 ± 1.6	6.6 ± 8.5
SGL	0.3 ± 0.7	0.2 ± 0.6	0.2 ± 0.6	0.6 ± 1.2	0.4 ± 0.8	4.6 ± 8.4
STR	0.0 ± 0.0	0.0 ± 0.0	0.0 ± 0.0	0.2 ± 0.9	1.6 ± 6.3	1.9 ± 3.7
NER	0.0 ± 0.0	0.0 ± 0.0	0.0 ± 0.0	0.0 ± 0.0	3.8 ± 15.0	1.2 ± 5.6

ARC-subCLST, sub-clusters based on architectural element; mean ± standard deviation is shown;

BAC, bronchioloalveolar; TUB, tubular; ACI, acinar; DCT, ductal; PAP, papillary; SOL, solid; TRB, trabecular; SGL, single; STR, striated; NER, neuroendocrinal.

Table 7. Postoperative recurrence rates and hazard ratios in high- and low-grade groups at stage IA

	Crude recurrence rate % [No.]	Hazard ratio [95% CI]
Cut-off 71.5%		
	P = 0.022	P = 0.002
Low -grade group [116]	3.4 [4]	1.00 [ref.]
High-grade group [13]	23.1 [3]	7.35 [1.64- 33.0]
Cut-off 9.5%		
	P = 0.058	P = 0.041
Low -grade group [66]	1.5 [1]	1.00 [ref.]
High-grade group [63]	9.5 [6]	6.72 [0.81- 55.79]

ARC-CLSTs, clusters based on architectural elements; No., number of cases;

P, P value for crude recurrence rate and hazard ratio are calculated by Fisher's exact test and Log-rank test, respectively; CI, confidence interval; ref., reference; N.A., not available

the sub-clusters (Table 5). Tumors of sub-clusters A1 and A2 predominantly affected females/non-smokers. In contrast, tumors of sub-clusters C2, and D mostly affected males/heavy smokers with a higher Brinkmann index (Table 5). Tumors of sub-cluster B almost evenly affected females/non-smokers and males/smokers (Table 5). These findings are consistent with notion that the postoperative performance of males/smokers is generally poorer [3,12] (Figure 6 and Table 4).

Concise criteria suitable for practical use

As described above, element of histological architecture was most significantly associated with a disease recurrence. However, its prognostic value was found only in cases of stage IA,

but not stage IB disease (Figure 6, Table 2 and Table 3). Thus, we thereafter focused on stage IA disease and tried to establish concise criteria suitable for practical use to subdivide cases into sub-groups with better and worse outcome. Reviewing proportions of architectural elements among the sub-clusters (Figure 7 and Table 6), those with a worse outcome (C2, and D) were found to mainly consist of ACN and/or SOL components, while those with a better outcome (A1, A2, B and C1) mainly consisted of BAC, PAP and/or TUB components (Figure 6, Figure 7, and Table 6). The findings led us to consider that a balance of low-grade (BAC, PAP and TUB) and high-grade (ACN and SOL) components could be important in determining postoperative outcome. A cut-off value, 71.5% of the high-grade component comprised by a tumor, was

calculated according to the area under the curve (AUC, 0.708) using a relative operating characteristic (ROC) curve (the proportion comprising the low-grade component was found not to be suitable for setting a threshold according to mathematical logic) (**Figure 8A** and **8B**). According to this cut-off, tumors (stage IA) were categorized into a high-grade group (tumors comprising more than or equal to 71.5% of the high component and a low-grade group (tumors comprising less than 71.5% of the high component). The groups exhibited a significant difference in postoperative outcome (**Figure 8C** and **Table 7**) [specificity 91.9%, sensitivity 42.9%]. Optionally, a cut-off value of 9.5% was set to obtain 80% sensitivity. The level of significance was decreased (**Figure 8D** and **Table 7**) and the specificity was inevitably affected [specificity 58.9%, sensitivity 80.0%].

Discussion

The main aim of the present study was to establish a practical sub-typing system for predicting postoperative outcome in cases of stage I ADC. We used the morphometric profiling. Possible differences in postoperative outcome among clusters based on multiple morphometric elements were analyzed. Histological architecture had the most prognostic value, especially in stage IA disease (**Figure 6**, **Table 2** and **Table 3**). The elements of histological architecture could be roughly categorized into low-grade (BAC, PAP and TUB) and high-grade (ACN and SOL) components. A cut-off value was determined as 71.5% of the high-grade component (**Figure 8** and **Table 7**). The sub-grouping system according to the cut-off is concise enough for practical use, however its sensitivity seems not satisfactory [specificity 91.9%, sensitivity 42.9%]. Eighty percent sensitivity requires a cut-off value of 9.0%, which affects specificity [specificity 58.9%, sensitivity 80.0%] (**Figure 8C**). We consider this could be the limit of the prognostic accuracy provided by morphological features of tumor parenchyma alone. Studies have demonstrated the excellent prognostic potential of the proportion of fibrotic area or of the status of fibrotic reactions in collapsed lesions in ADC with a BAC component [4,7,14]. Moreover, certain molecular genetic alterations in tumor cells were reported to closely associate with postoperative outcome in cases of stage I ADC [10,15]. Therefore, we are interested in combining such factors with our sub-grouping system to further

improve its accuracy.

In summary, the present study has confirmed mathematically that histological architecture is the most important morphological feature of tumor parenchyma, and has proposed a concise sub-grouping system (cut-off value, 71.5% (practically 70%) of the high grade component (ACN or SOL)) for predicting postoperative recurrences in cases of stage I, especially stage IA, ADC. Importantly, we have subdivided the acinar pattern of the traditional classification system [2] into "TUB", which is defined as a tubular or glandular structure lined with single-layered neoplastic cells, and "ACN", which is defined as a tubular or glandular structure lined with poly-layered neoplastic cells or as a fused glandular structure such as the cribriform pattern, and also demonstrated their utility. This proposal is worthy of note. We hope our efforts will aid in improving the histopathologic classification of ADC.

Acknowledgements

This work was supported by the Japanese Ministry of Education, Culture, Sports, and Science (Tokyo Japan), the Smoking Research Foundation (Tokyo, Japan), and by a grant from Yokohama Medical Facility (Yokohama, Japan). We especially thank Masaichi IKEDA (Department of Pathology, Yokohama City University Graduate School of Medicine) and Shigeko IWANADE and Emi HONDA (Division of Pathology, Kanagawa Prefectural Cardiovascular and Respiratory Center Hospital) for technical assistance.

Please address correspondence to: Hitoshi Kitamura, MD, Department of Pathology, Yokohama City University Graduate School of Medicine, 3-9, Fukuura, Kanazawa-ku, 236-0004, Yokohama, Japan. Tel: +81-45-787-2583, Fax: +81-45-789-0588, E-mail: pathola@med.yokohama-cu.ac.jp

References

- [1] Spira A, Ettinger DS. Multidisciplinary management of lung cancer. *N Engl J Med* 2004;350:379-392.
- [2] Travis WD, Brambilla E, Muller-Hermelink HK, Harris CC (Eds). *World Health Organization Classification of Tumors. Pathology and Genetics of the Lung, Pleura, Thymus and Heart*, IARC Press, Lyon, 2004.
- [3] Asamura H, Goya T, Koshiishi Y, Sohara Y, Egu-

Improved histological subtyping of lung adenocarcinoma

- chi K, Mori M, et al. A Japanese lung cancer registry study: prognosis of 13,010 resected lung cancers. *J Thorac Oncol* 2008;3:46-52.
- [4] Noguchi M, Morikawa A, Kawasaki M, Matsuno Y, Yamada T, Hirohashi S et al. Small adenocarcinoma of the lung. Histologic characteristics and prognosis. *Cancer*. 1995;75:2844-2852.
- [5] Ou SH, Zell JA, Ziogas A, Anton-Culver H. Prognostic factors for survival of stage I non-small cell lung cancer patients: a population-based analysis of 19,702 stage I patients in the California cancer registry from 1989 to 2003. *Cancer*. 2007;110:1532-1541.
- [6] Tsuchiya T, Akamine S, Muraoka M, Kamohara R, Tsuji K, Urabe S, et al. Stage IA non-small cell lung cancer: Vessel invasion is a poor prognostic factor and a new target of adjuvant chemotherapy. *Lung Cancer* 2007;56:341-348.
- [7] Yokose T, Suzuki K, Nagai K, Nishiwaki Y, Sasaki S, Ochiai A. Favorable and unfavorable morphological prognostic factors in peripheral adenocarcinoma of the lung 3 cm or less in diameter. *Lung Cancer*. 2000;29:179-188.
- [8] Hamada C, Tanaka F, Ohta M, Fujimura S, Kodama K, Imaizumi M, Wada H. Meta-analysis of postoperative adjuvant chemotherapy with tegafur-uracil in non-small-cell lung cancer. *J Clin Oncol* 2005;23:4999-5006.
- [9] Kato H, Ichinose Y, Ohta M, Hata E, Tsubota N, Tada H, et al. A randomized trial of adjuvant chemotherapy with uracil-tegafur for adenocarcinoma of the lung. *N Engl J Med* 2004;350:1713-1721.
- [10] Okudela K, Woo T, Mitsui H, Yazawa T, Shimoyamda H, Tajiri M, et al. Morphometric Profiling of Lung Cancers – its association with clinicopathologic, biological and molecular genetic features -. *Am J Surg Pathol*. 2010 in press [doi: 10.1097/PAS.0b013e3181c79a6f]
- [11] Mountain CF. Revisions in the international system for staging lung cancer. *Chest*. 1997;111:1710-1717.
- [12] Bertheau P, Cazals-Hatem D, Meignin V, Roquan-court A, Verola O, Lesourd A, et al. Variability of immunohistochemical reactivity on stored paraffin slides. *J Clin Pathol* 1998;51:370-374.
- [13] DiVito KA, Charette LA, Rimm DL, Camp RL. Long-term preservation of antigenicity on tissue microarrays. *Lab Invest* 2004;84:1071-1078.
- [14] Suzuki K, Yokose T, Yoshida J, Nishimura M, Takahashi K, Nagai K, et al. Prognostic significance of the size of central fibrosis in peripheral adenocarcinoma of the lung. *Ann Thorac Surg*. 2000;69:893-897.
- [15] Woo T, Okudela K, Yazawa T, Wada N, Ogawa N, Ishiwa N, et al. Prognostic value of KRAS mutations and Ki-67 expression in stage I lung adenocarcinomas. *Lung Cancer*. 2009;65:355-62.